https://doi.org/10.5194/egusphere-2023-399
Preprint. Discussion started: 17 March 2023

Hysteresis and orbital pacing of the early Cenozoic Antarctic ice sheet

Jonas Van Breedam[1], Philippe Huybrechts[1], Michel Crucifix[2]

[1]Earth System Science & Departement Geografie, Vrije Universiteit Brussel, Brussels, Belgium
[2]Earth and Life Institute, Université Catholique de Louvain, Louvain-la-Neuve, Belgium

Correspondence to: Jonas Van Breedam (jonas.van.breedam@vub.be)

Abstract. The hysteresis behaviour of ice sheets arises because of the different thresholds for growth and decline of a continental-scale ice sheet depending on the initial conditions. In this study, the hysteresis effect of the early Cenozoic Antarctic ice sheet is investigated with an improved ice sheet-climate coupling method that accurately captures the ice-albedo feedback. It is shown that the hysteresis effect of the early Cenozoic Antarctic ice sheet is about ~180 ppmv or between 3.5˚C and 5.5˚C, depending only weakly on the bedrock elevation dataset. Excluding the solid Earth feedback decreases the hysteresis effect significantly towards ~40 ppmv, because the transition to a glacial state can occur at a higher forcing. The rapid transition from a glacial to a deglacial state and oppositely from deglacial to glacial conditions is strongly enhanced by the ice-albedo feedback, in combination with the elevation - surface mass balance feedback. Variations in the orbital parameters show that extreme values of the orbital parameters are able to exceed the threshold in summer insolation to induce a (de)glaciation. It appears that the long-term eccentricity cycle has a large influence on the ice sheet growth and decline and is able to pace the ice sheet evolution for constant CO_2 concentration close to the glaciation threshold.

1 Introduction

Nonlinear dynamics in the cryosphere are a source of large concern, with the possible collapse of the West-Antarctic ice sheet (Rosier et al., 2021) and the Greenland ice sheet (Boers and Rypdal, 2021). These so-called tipping points are thresholds beyond which self-reinforcing feedbacks could irreversibly lead to a new state (Lenton et al., 2019; Armstrong McKay et al., 2022). These thresholds might trigger other tipping points and could result in a tipping cascade (Klose et al., 2020). For instance, melting of the Greenland ice sheet could halve the strength of the thermohaline circulation in the North Atlantic when large amounts of meltwater are released from the ice sheet (Van Breedam et al., 2020).

The build-up of the Antarctic ice sheet around the Eocene-Oligocene Transition (EOT) is also a tipping point and occurred at a time that environmental conditions were favourable for ice sheet growth, ensuring a series of positive feedbacks, eventually leading to the formation of a large ice sheet. These favourable environmental conditions included the thermal insulation of

https://doi.org/10.5194/egusphere-2023-399
Preprint. Discussion started: 17 March 2023

Antarctica by either ocean currents (Kennett, 1977), wind patterns (Houben et al., 2019), or both; the decline in carbon dioxide concentrations (Pagani et al., 2011); and tectonic activity that moved the Antarctic continent closer to the South Pole.

Once environmental conditions are optimal for ice sheet growth, a small change in climate conditions can trigger a large, nonlinear response. It is generally believed that orbital parameter variations are the cause of large ice sheet changes and have regulated ice sheet growth and decline during almost any geological period in the history of the Earth (Mitchell et al., 2021). These interpretations arise from the identification of periodic events observed in geological archives and are attributed to reflect Milankovitch cycles (De Vleeschouwer et al., 2017). The main influence of changes in the orbital parameters on the climate system is a seasonal and latitudinal redistribution of incoming solar radiation. The different orbital parameters each have a different periodicity. The precession has periods of 19 and 23 kyr, the obliquity of 41 kyr and the eccentricity has periods around 100 kyr and 405 kyr (Laskar et al., 2011). Especially the eccentricity has been thought to play a crucial role on the ice sheet stability (Horton et al., 2012).

Hysteresis is the dependence of a physical system based on its history. The ice sheet-climate system exhibits hysteresis where for a given forcing, either a large ice sheet or a small ice sheet/bare bedrock are stable states. Which one is reached depends on the initial conditions. For instance, when CO_2 concentrations are very low, a large continental ice sheet can exist and it will be far from a tipping point (Figure 1). As CO_2 concentrations (control parameter) increase, the system gets closer to a tipping point and will eventually make an abrupt change towards a new system state without the ice sheet. The underlying mechanisms to induce the non-linear changes are the ice-albedo feedback and the elevation-surface mass balance feedback.

In previous work, the hysteresis behaviour of ice sheets has been investigated to determine the future thresholds for ice sheet stability of the Greenland ice sheet (Letréguilly et al., 1991; Ridley et al., 2005; Ridley et al., 2010; Robinson et al., 2012; Levermann and Winkelmann, 2016) and the Antarctic ice sheet (Huybrechts, 1994b; Garbe et al., 2020). Hysteresis of ice sheet volume variations has been identified during the Quaternary ice ages to explain the 100 kyr cyclicity of prolonged ice sheet build-up and rapid deglaciation (Calov and Ganopolski, 2005; Abe-Ouchi et al., 2013).

Pollard and Deconto (2005) determined the hysteresis of the early Antarctic ice sheet at the Eocene-Oligocene transition with a set of idealised orbital parameters and a matrix method where a limited number of climate model runs were performed based on end members in the forcing. The adopted approach captured the important height-mass balance feedback. However, the ice-albedo feedback may not have been properly taken into account, given the small set of initial ice sheet geometries used in that study. Furthermore, beyond the positive height-mass balance and ice-albedo feedbacks, a negative feedback from the solid Earth might arise during the build-up and decline of a continental scale ice sheet (Crucifix et al., 2001). The solid Earth will deflect in response to ice mass loading and as a result, the surface elevation increase due to increased accumulation of ice will

https://doi.org/10.5194/egusphere-2023-399
Preprint. Discussion started: 17 March 2023

be delayed. It is proposed that this negative feedback also delays grounding line migration in the marine sectors of Antarctica, for instance during the coming centuries (Larour et al., 2019).

In this study, the hysteresis for the early Cenozoic Antarctic ice sheet is tested with an improved methodology, based on an emulator calibrated on 20 predefined ice sheet geometries. This number of different ice sheet geometries allows the climate model to represent the climatic state for a small change in the surface type. This way, the albedo effect from a change in ice sheet area is well-captured. The sensitivity of the threshold behaviour is tested to different recent bedrock elevation reconstructions. Since the solid Earth rebound feedback has a potential significant impact on the glaciation threshold, sensitivity tests are performed to assess the strength of the isostatic adjustment feedback on the ice sheet growth. Additionally, the importance of the orbital parameters on the threshold is investigated for a series of constant CO_2 curves, keeping one of the orbital parameters constant at a time to disentangle the threshold dependency for a given combination of orbital parameters and CO_2 concentrations. Since geological evidence pointed to ephemeral glaciations prior to the EOT (Scher et al., 2014; Carter et al., 2017), this study aims to identify the forcing needed to initiate and end a continental-scale glaciation.

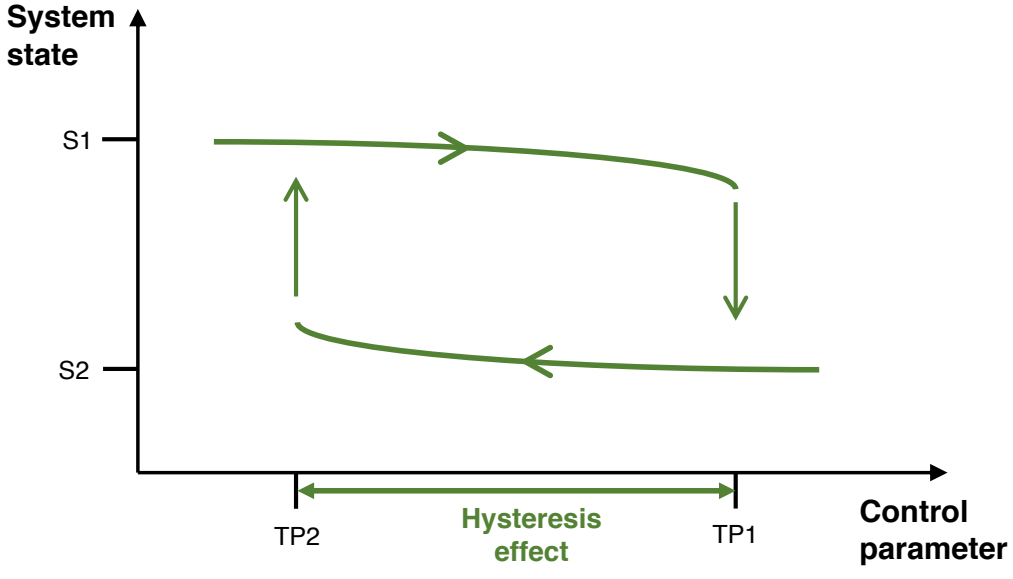

Figure 1: Typical diagram visualizing the concept of the hysteresis effect. The system state is either a continental-scale ice sheet (S1) or no ice sheet (S2). The control parameter can be the surface temperature or the forcing itself such as the CO_2 forcing or the insolation forcing. TP1 and TP2 represent tipping points at which the system can quickly change its state.

https://doi.org/10.5194/egusphere-2023-399
Preprint. Discussion started: 17 March 2023

2 Model description and experimental set-up

The different models used in this study are the climate model HadSM3 and the ice sheet model AISMPALEO. The models interact with one another through the Gaussian process emulator CLISEMv1.0 (Van Breedam et al., 2021b).

2.1 Antarctic ice sheet model AISMPALEO

The three-dimensional thermomechanical ice sheet model AISMPALEO is used at a resolution of 40 km. Grounded ice flow is calculated using the Shallow Ice Approximation, while ice shelf flow is derived from the Shallow Shelf Approximation. Grounded ice flow is a result from internal deformation and basal sliding at locations where the pressure melting point is reached (Huybrechts and de Wolde, 1999). All stress components between the grounded ice and the floating ice are considered in a one grid cell wide transition zone. Ice shelves are developing when the grounded ice reaches the coast and the influx of ice exceeds the sum of surface ablation and basal melting. The mass balance is computed using the efficient PDD model (Janssens and Huybrechts, 2000). The PDD model uses the yearly sum of the mean daily temperatures above 0˚C to determine the melt potential. Random weather fluctuations and the daily cycle in temperature are taken into account by including a standard deviation of the mean daily temperature of 4.2˚C. Different DDFs are used to melt snow and ice, respectively 0.003 m i.e. $^{\circ}C^{-1}$ day^{-1} and 0.008 m i.e. $^{\circ}C^{-1}$ day^{-1}. The melt rate is computed by multiplying the DDFs of snow and ice with the sum of the PDDs. The difference between snow and rain is calculated based on a surface temperature threshold of 1˚C. When ice is melting, part of the meltwater can be retained or refreeze in the snowpack to form superimposed ice. The model includes a component to calculate the solid Earth response due to ice mass addition and removal. The isostatic model consists of an elastic lithosphere with a certain flexural rigidity on top of a viscous asthenosphere, to allow the crust to deform far beyond the local ice loading (Huybrechts, 2002).

2.2 Climate model HadSM3

The coupled atmosphere-slab ocean climate model HadSM3 (Williams et al., 2001) provides the climatic fields. The resolution of the atmospheric component is 2.5˚ for the latitude and 3.75˚ for the longitude. It has a hybrid vertical coordinate with 19 levels in the vertical (Pope et al., 2000). The heat fluxes between the surface and the atmosphere are calculated with the MOSES-1 scheme (Cox et al., 1999). The slab ocean model equilibrates with the atmosphere in a 50 m thick layer. Monthly variable, zonal mean sea surface temperatures (SSTs), representative for the late Eocene (Evans et al., 2018), are prescribed to calibrate the anomalous heat convergence. These heat fluxes, representative for the horizontal heat transport and seasonal deep-water exchange, are then used to simulate realistic sea surface temperatures under various climate conditions. Sea-ice is simulated during the winter months and is mostly constrained to the Weddell Sea region, but disappears again during the austral summer in most simulations. The palaeogeographic reconstruction is based on the method presented in Baatsen et al.

https://doi.org/10.5194/egusphere-2023-399
Preprint. Discussion started: 17 March 2023

(2016) using the van Hinsbergen et al. (2015) plate rotational model. The bedrock topography comes from Wilson et al. (2012) and is representative for the Eocene-Oligocene transition (EOT) at 34 Ma (Figure 2).

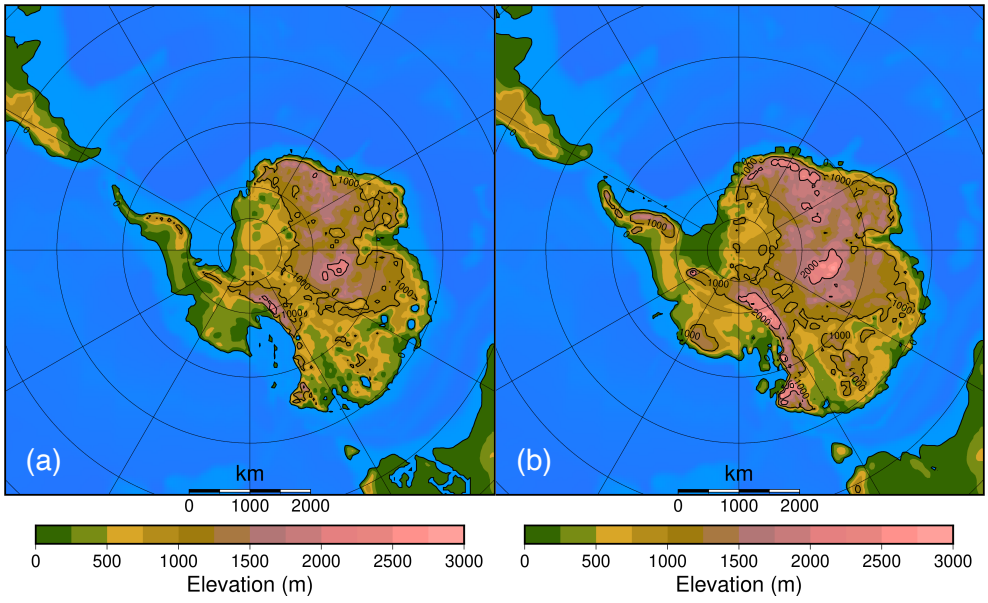

Figure 2: (a) Minimum and (b) maximum bedrock elevation reconstructions from Wilson et al. (2012).

2.3 Emulator CLISEMv1.0

The emulator CLISEMv1.0 (Van Breedam et al., 2021b) is used to force the ice sheet model during the multi-million-year simulations. The emulator is calibrated on 100 climate model runs from HadSM3, which is forced with a unique combination of the orbital parameter ε (obliquity) and the parameter combinations $esin\varpi$ and $ecos\varpi$, where e is the eccentricity and ϖ is the longitude of the perihelion. The 100 model runs also sample 20 different ice sheet geometries, ranging from a very small ice cap in the Gamburtsev mountains up to a fully glaciated Antarctic ice sheet. The geometries have been chosen such that their ice volumes have a good spread between the smallest and the largest ice sheet geometries. The CO_2 forcing across the runs ranges from 550 ppmv to 1150 ppmv. After the calibration and validation process (see for details Van Breedam et al., 2021a), the emulator is able to provide the climatic forcing (temperature and precipitation fields) necessary to drive the mass balance of AISMPALEO. The emulator set-up is the same as EMULATOR_20 calibrated on ice volume as presented in Van Breedam et al (2021a), which has been applied to the late Eocene to investigate the potential for late Eocene glaciations (Van Breedam et al., 2022). The climatic fields are updated each 500 years in the ice sheet model, a time-step that is sufficient to capture the feedbacks between the ice sheet and the external forcing.

https://doi.org/10.5194/egusphere-2023-399
Preprint. Discussion started: 17 March 2023

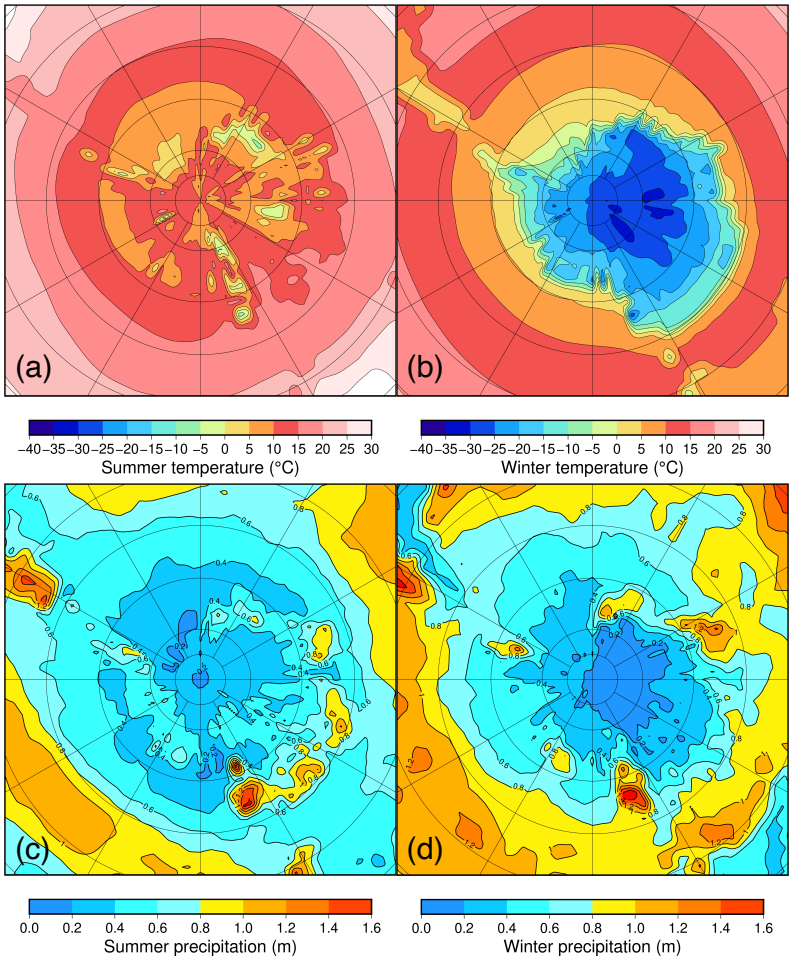

Figure 3: Antarctic climatologies for a 2x pre-industrial CO_2 forcing. (a) Summer (DJF) temperature. (b) Winter (JJA) temperature. (c) Summer (DJF) precipitation. (d) Winter (JJA) precipitation.

The simulated Antarctic climate is strongly dependent on the forcing. The seasonal temperature and precipitation patterns are shown for a nearly ice-free Antarctica (only ice on the highest elevations; Figure 3). The CO_2 forcing is representative for a 2x pre-industrial CO_2 forcing (560 ppmv), the obliquity is close to the present-day obliquity with 23.4˚, the eccentricity is small (0.007) resulting in an almost circular orbit and therefore, the effect of the precession is negligible. The precipitation is largest along the Antarctic continental margin and decreases land inwards. There is a lower precipitation rate during the austral winter (June-July-August or JJA) than during the austral summer (December-January-Februari or DJF) above the Antarctic continent. The seasonality is extremely large on the Antarctic continent with a winter-summer difference in mean daily temperatures of 30-35 ˚C along the continental margin and up to 50-55˚C in the interior of the continent close to the South Pole. This is in line with the study from Baatsen et al. (2020) using CESM 1.0.5, who identified a large seasonality of 35-45˚C on the Antarctic continent and a monsoonal type of climate with larger summer precipitation.

https://doi.org/10.5194/egusphere-2023-399
Preprint. Discussion started: 17 March 2023

2.4 Experimental design

All simulations span the time period between 40 Ma and 30 Ma, for which the orbital forcing for the different simulations is provided. The simulations that start from a bare bedrock are forced with an atmospheric CO_2 concentration linearly decreasing from 1150 ppmv to 550 ppmv. The CO_2 forcing is reversed for the simulations that start from a continental scale ice sheet with a linearly increasing CO_2 concentration from 550 ppmv to 1150 ppmv (Table 1). The lower and upper bounds of the CO_2 concentration are chosen to include a forcing when either the ice sheet grows to a continental scale for any astronomical forcing (550 ppmv) and a forcing that is too high to allow for any ice sheet to exist (1150 ppm).

Table 1: Standard set of experiments with the Wilson minimum and Wilson maximum bedrock topography as boundary conditions and variable orbital forcing.

	Ice level (at start)	CO_2 (ppmv)	eccentricity	obliquity
Wilson minimum	Ice	1150 to 550 (linear)	variable	variable
Wilson minimum	No ice	550 to 1150 (linear)	variable	variable
Wilson maximum	Ice	1150 to 550 (linear)	variable	variable
Wilson maximum	No ice	550 to 1150 (linear)	variable	variable

The orbital forcing is included to investigate the influence of the insolation thresholds for ice sheet growth and decline in detail. In these runs, the individual orbital parameters or the insolation are the control parameters (see Figure 1 and Table 2) and the CO_2 concentrations are kept constant with values close to the glaciation threshold. The orbital parameter solution La2010 from Laskar et al. (2011) is used (Figure 4). The orbital parameters contain periods ranging from about 20 kyr for the precession up to 405 kyr for the long-term cycle in the eccentricity. On a multi-million-year timescale, the eccentricity also exhibits variations with a longer period. Spectral analyses reveals that this cycle has a main periodicity of 2.4 Ma (Laskar et al., 2004). The duration of the experiments where the influence of the orbital parameters is investigated is 2.4 Myr long starting at 34.2 Ma up to 31.8 Ma to capture the extrema when the 100 kyr, 405 kyr and 2.4 Ma cycles reach a maximum, separately and combined.

Because the initial bedrock topography has a large influence on the ice sheet initiation and also on the size of the continental scale ice sheet, simulations are performed for the minimum and maximum bedrock topography estimate from Wilson et al. (2012) in order to test the hysteresis and threshold behaviour for two extremes (Figure 2). The simulations start from a bare bedrock topography and the atmospheric CO_2 concentrations are linearly decreasing to induce the continental scale glaciation. The resulting continental scale ice sheet extent is then used for the simulations starting from a glaciated continent.

https://doi.org/10.5194/egusphere-2023-399
Preprint. Discussion started: 17 March 2023

Table 2: Experiment overview for the runs investigating the influence of the orbital parameters for fixed CO_2 concentration levels.

	Ice level (at start)	CO_2 (ppmv)	eccentricity	obliquity
Wilson maximum	Ice	650, 700, 750, 800, 850, 900, 950, 1000, 1050, 1100, 1150	0.01, 0.02, 0.03, 0.04, 0.05, 0.06	variable
Wilson maximum	No ice	650, 700, 750, 800, 850, 900, 950, 1000, 1050, 1100, 1150	0.01, 0.02, 0.03, 0.04, 0.05, 0.06	variable
Wilson maximum	Ice	600, 650, 700, 750, 800, 850, 900, 950, 1000, 1050, 1100, 1150	variable	22.5°, 23°, 23.5°, 24°, 24.5°
Wilson maximum	No ice	600, 650, 700, 750, 800, 850, 900, 950, 1000, 1050, 1100, 1150	variable	22.5°, 23°, 23.5°, 24°, 24.5°

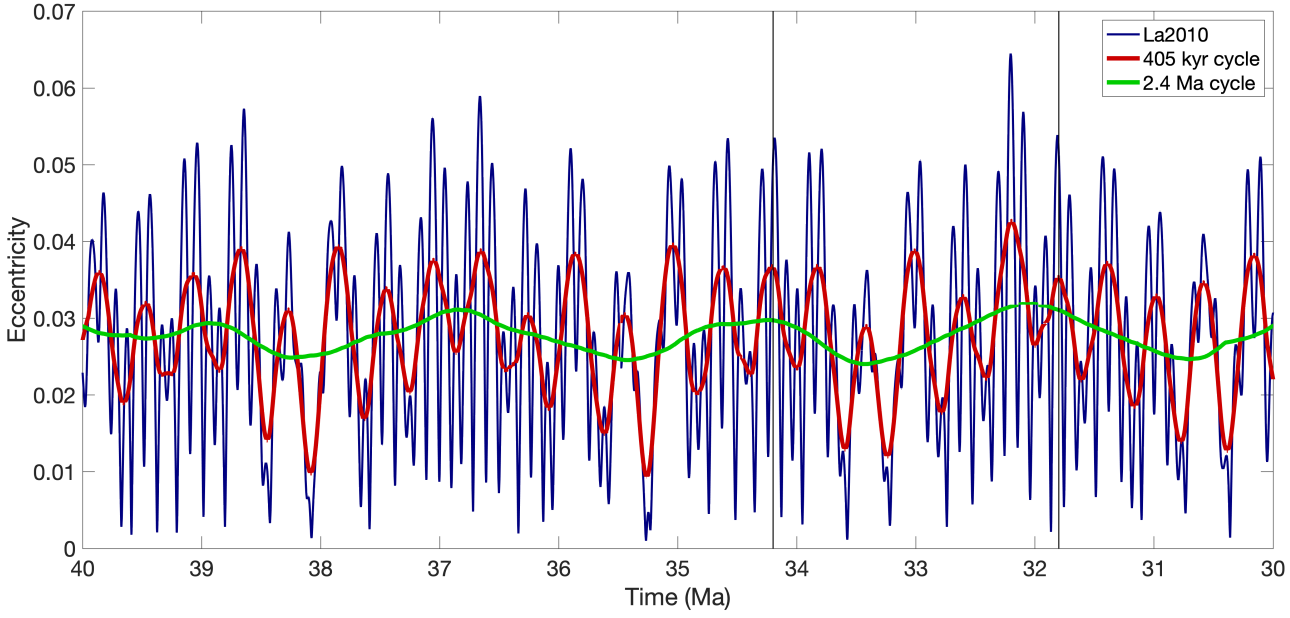

Figure 4: Earth's orbital eccentricity between 40 Ma and 30 Ma using the La2010 orbital solution (Laskar et al., 2011). The ~100 kyr cycle (blue) is clearly visible. The 405 kyr cycle (red) and 2.4 Ma cycle (green) are visualized by applying a running mean on the eccentricity from the La2010 solution. The period between 34.2 Ma and 31.8 Ma indicates one 2.4 Myr period in eccentricity at around the EOT.

https://doi.org/10.5194/egusphere-2023-399
Preprint. Discussion started: 17 March 2023

3 Ice sheet hysteresis

The thresholds for glaciation and deglaciation are dependent on the bedrock topography, because of its influence on the surface temperature. First, in section 3.1 the sensitivity of the Antarctic ice sheet hysteresis is tested to the initial bedrock topography dataset. Additionally, the influence of the solid Earth feedback that causes isostatic depression during the build-up of an ice sheet is quantified in section 3.2.

3.1 Sensitivity to the bedrock topography dataset

Antarctic continental scale glaciation is strongly sensitive to the applied bedrock topography dataset. Fig. 5 shows that the CO_2 concentration threshold to initiate Antarctic glaciation is higher when the bedrock topography is higher with a value of 870 ppmv for the maximum bedrock topography reconstruction and a value of 650 ppmv for the minimum bedrock topography reconstruction. This is a logical consequence of the temperature decrease with elevation. The snowline will intersect the topography more easily for higher CO_2 values when the initial bedrock topography is higher. The same is true for the ice sheet's decline. The higher the initial bedrock topography, the larger the area of the continental scale ice sheet. Except for the larger area, the ice sheet elevation is also higher. The mean annual surface temperature (MAT_sur), defined here as the mean for all the land-based and ice-covered grid points, is lower above the ice sheet because of the higher elevation. Hence, to melt a continental scale ice sheet with a larger area and a higher surface elevation, the CO_2 concentration must also be higher. On the other hand, the difference in the CO_2 threshold or the hysteresis effect between glaciation and deglaciation does not depend much on the bedrock topography. For the Wilson maximum topography, the CO_2 threshold difference between glaciation and deglaciation is about 180 ppmv, while the threshold is 170 ppmv for the Wilson minimum topography.

The difference between the glaciation and deglaciation thresholds can also be expressed in terms of a temperature change. Grounding line retreat for marine-based ice sheets can be initiated by subsurface melting of ice shelves, but melting of a continental scale ice sheet is mostly governed by changes in the surface mass balance. Hence, the surface temperature is key in determining the threshold at which the ice sheet starts to grow or when the deglaciation occurs. The spatial MAT_sur ranges from -5˚C at the ice sheet margin to -45˚C and -50˚C in East Antarctica for respectively the Wilson minimum and Wilson maximum bedrock topography. The colder temperatures for the Wilson maximum topography are mainly due to the differences in surface elevation (Figure 6). These temperatures are reached for a CO_2 forcing of 550 ppmv and are still about 10-20˚C higher than the temperatures over the present-day Antarctic ice sheet.

https://doi.org/10.5194/egusphere-2023-399
Preprint. Discussion started: 17 March 2023

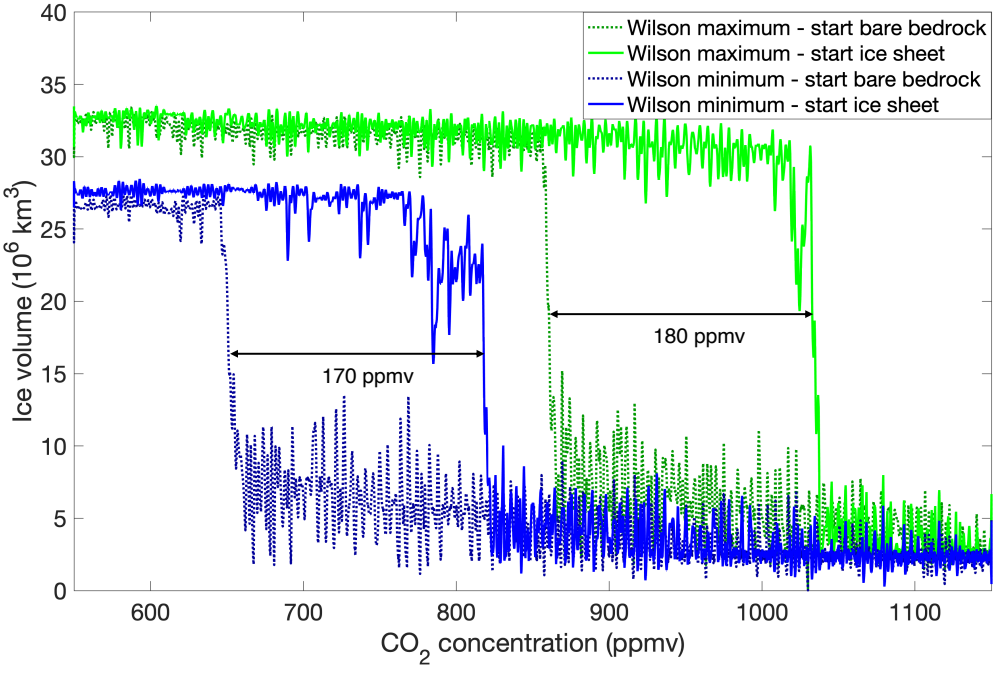

Figure 5: Hysteresis behaviour of ice sheet growth and decline for linearly varying CO_2 concentrations between 550 ppmv and 1150 ppmv for the Wilson maximum bedrock topography (green) and the Wilson minimum bedrock topography (blue) reconstructions. The dotted lines represent simulations that start from a bare bedrock topography. The solid lines represent simulations that start from a continental-scale ice sheet.

https://doi.org/10.5194/egusphere-2023-399
Preprint. Discussion started: 17 March 2023

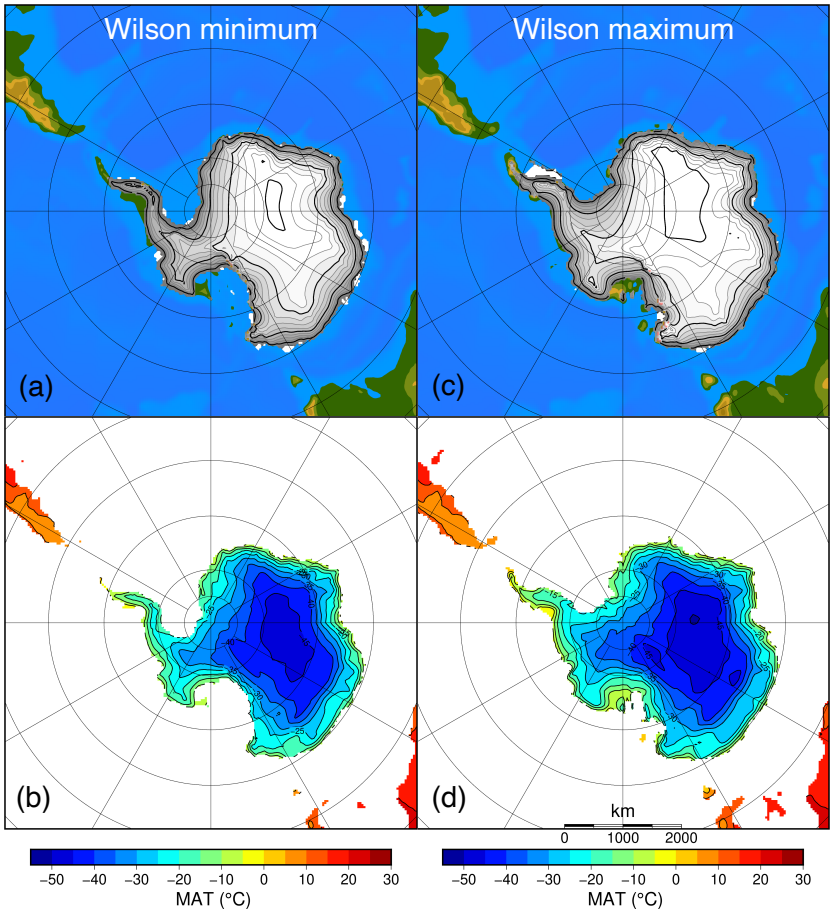

Figure 6: Continental-scale ice sheet geometry for the (a) Wilson minimum bedrock topography and (b) the corresponding spatially varying mean annual surface temperature and for (c) the Wilson maximum bedrock topography and (d) the corresponding spatially varying mean annual surface temperature.

https://doi.org/10.5194/egusphere-2023-399
Preprint. Discussion started: 17 March 2023

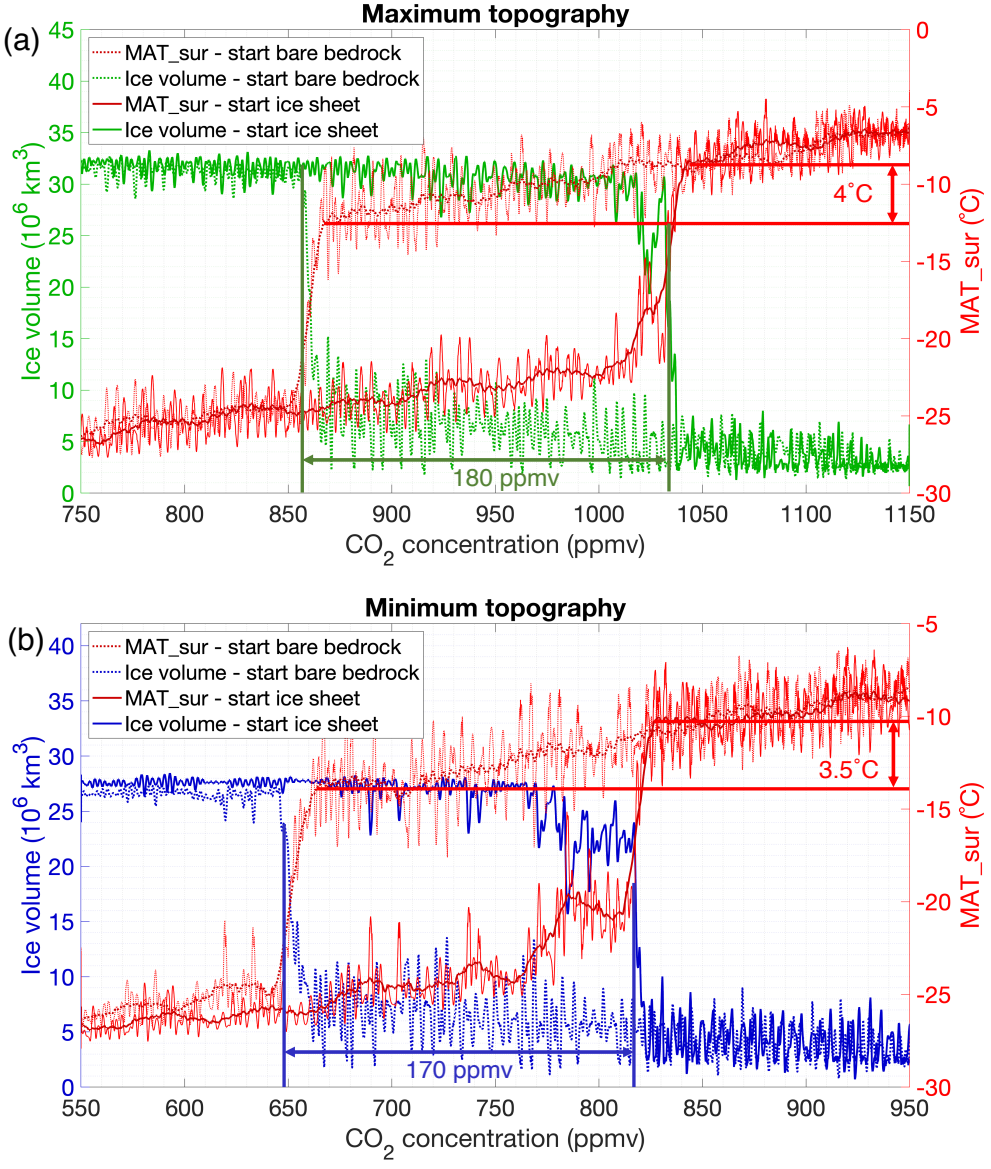

Figure 7: Mean annual temperature change (MAT_sur) and ice volume evolution using (a) the Wilson maximum bedrock topography and (b) the Wilson minimum bedrock topography. The simulation starts either from a bare bedrock and a CO_2 forcing of 1150 ppmv that linearly decreases towards 550 ppmv or from a continental scale ice sheet and a CO_2 forcing of 550 ppmv that linearly increases towards 1150 ppmv.

The MAT_sur for a deglaciated Antarctic continent at 1150 ppmv is about -7˚C during the late Eocene for the rebounded Wilson maximum bedrock topography (Figure 7a) and slightly higher with -6˚C for the Wilson minimum bedrock topography (Figure 7b). The annual march in temperatures is about 30˚C with a mean January temperature of 13˚C and a mean July

https://doi.org/10.5194/egusphere-2023-399
Preprint. Discussion started: 17 March 2023

temperature of -17˚C (not shown). This indicates that in winter time snow accumulates, while it melts again in summer. The MAT_sur needs to be lower to cause a full glaciation, with ~6˚C and ~8˚C respectively for the Wilson maximum and minimum bedrock topography. Temperatures range from -26˚C to -29˚C for the Wilson minimum and the Wilson maximum bedrock topography at a CO_2 concentration of 550 ppmv for a fully glaciated continent. To make the transition back to a deglaciated continent, the MAT_sur needs to rise above -20˚C (Figure 7).

For the Wilson minimum bedrock topography, the MAT_sur above the Antarctic continent is -14˚C when the entire continent is glaciated starting from a bare bedrock. Starting from a fully glaciated continent, the ice sheet deglaciates when the MAT_sur reaches -10˚C. For the Wilson maximum bedrock topography, these temperatures are very similar with a MAT_sur of -13˚C when the entire continent is glaciated starting from a bare bedrock and deglaciation starts when the MAT_sur reaches -9˚C. This indicates again that the hysteresis effect is independent of the particular bedrock elevation dataset. The hysteresis effect, expressed in terms of the MAT_sur threshold between glaciation and deglaciation, is about 4˚C.

3.2 Influence of the solid Earth rebound

It is thought that the solid Earth rebound (isostasy) provides a negative feedback to ice sheet growth. During the build-up of the ice sheet, the ice mass interacts with the lithosphere and deflects the underlying bedrock. Hence, the ice sheet elevation will not rise as fast and the lowering of the snowline (because of the gradual cooling in this experiment) will be delayed. The magnitude of this feedback is determined by performing experiments in which isostatic rebound is not considered.

The hysteresis effect in terms of the CO_2 forcing is much less pronounced when the solid Earth rebound feedback is neglected. The ice sheet decline occurs for a similar threshold of about 1080 ppmv when the solid Earth rebound is not taken into account (Figure 8). This is mainly a consequence of the ice-albedo feedback that is similarly strong in both the experiment with isostasy and without isostasy because the area of the continental scale ice sheet is the same regardless of the inclusion of the solid Earth feedback. The maximum height of the equilibrated continental-scale ice sheet is about 160 m higher without solid Earth feedback. This small difference in elevation does not have an impact on the CO_2 threshold to induce the deglaciation.

Without considering isostasy, ice sheet growth occurs already at a much higher CO_2 concentration of 980 ppmv (compared to 850 ppmv for the simulation including the solid Earth feedback) due to the rapid increase of the surface elevation when snow accumulates. Aside from the much higher surface elevation (up to 800 m higher) prior to the glaciation threshold, also the ice sheet area is about twice the size when excluding the solid Earth rebound. The hysteresis effect with respect to the CO_2 forcing is only 40 ppmv in this case. The MAT_sur threshold to glaciation is again about -13˚C, exactly the same temperature threshold as the experiment including the solid Earth rebound feedback. As already stated, this is a consequence of the higher surface

https://doi.org/10.5194/egusphere-2023-399
Preprint. Discussion started: 17 March 2023

260 elevation when snow and ice accumulate. The deglaciated continent has a MAT_sur of -6˚C, because of the smaller ice sheet geometry and generally lower surface elevation (Figure 9).

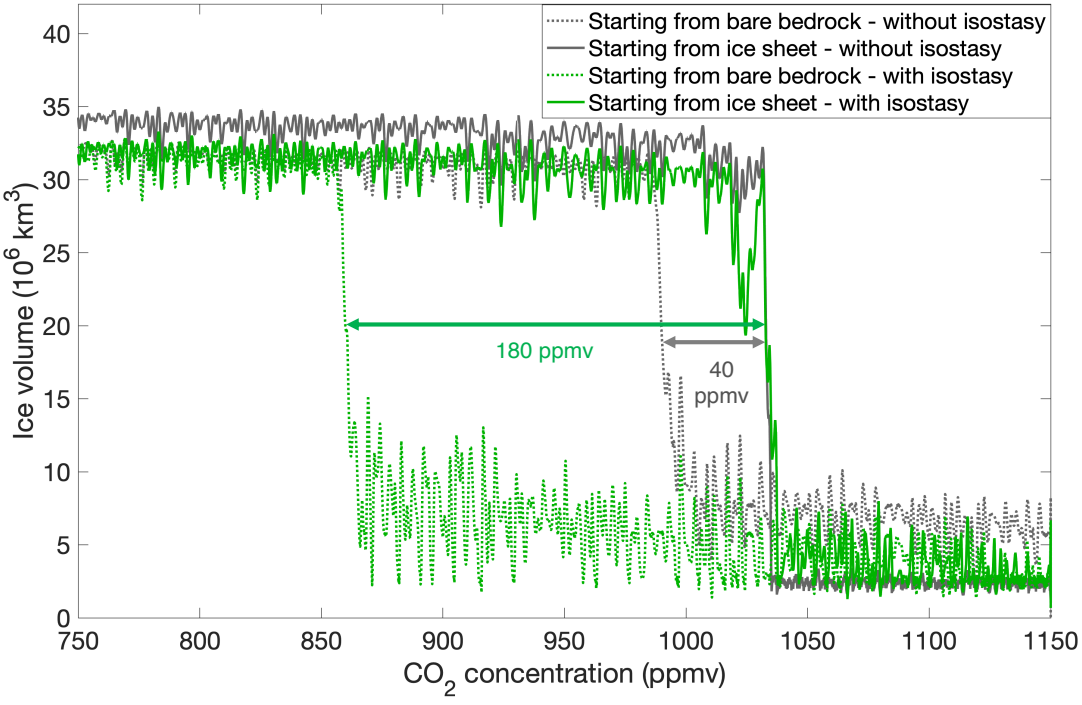

Figure 8: Ice sheet growth and decline for linearly decreasing/increasing CO_2 concentrations from 750 ppmv to 1150
265 **ppmv for the Wilson maximum bedrock topography reconstruction. The grey lines represent the ice sheet evolution for the simulations excluding the solid Earth rebound and the green lines represent the ice sheet evolution with solid Earth feedback.**

https://doi.org/10.5194/egusphere-2023-399
Preprint. Discussion started: 17 March 2023

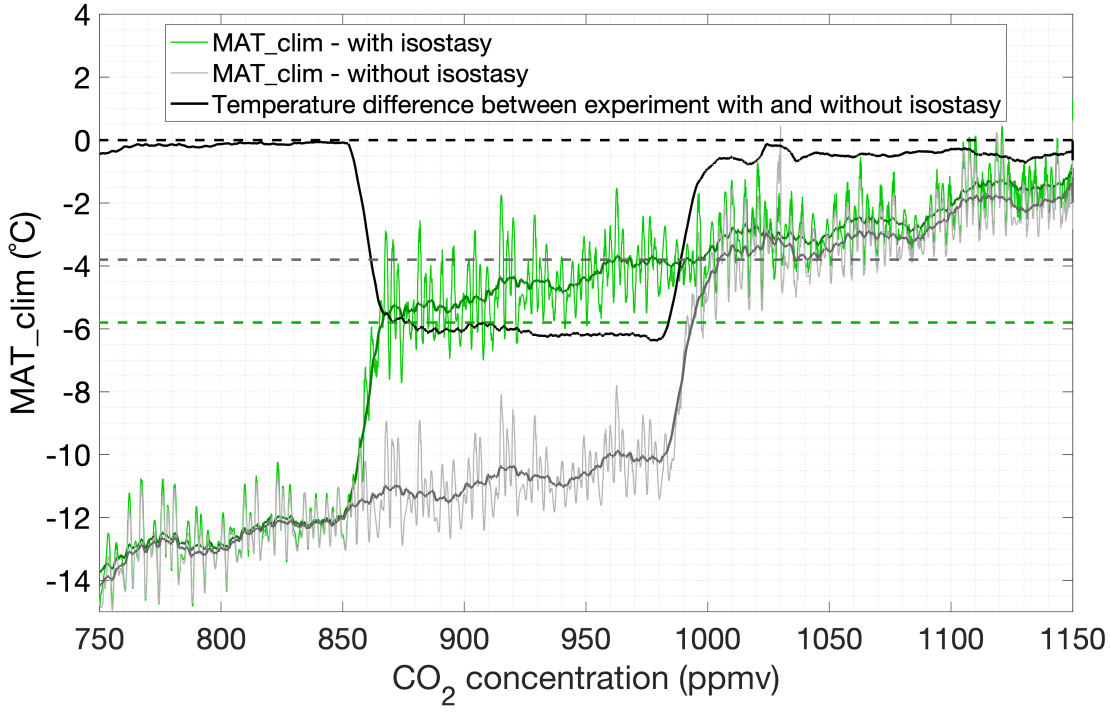

Figure 9: Elevation corrected mean annual temperature (MAT_clim) above the Antarctic continent. The simulations start from a bare bedrock and either include the solid Earth rebound feedback (green) or exclude the solid Earth rebound feedback (grey). The black dashed horizontal line indicates no temperature difference between the experiment including or excluding isostasy. The green and grey horizontal dashed lines indicate the MAT thresholds at which the Antarctic ice sheet grows to a continental scale.

The temperature threshold to glaciation and deglaciation is very similar between the experiments that include the isostatic rebound and the experiments that exclude isostasy. To disentangle the influence of the surface elevation, the MAT_sur is corrected for the surface elevation change by applying a constant lapse rate correction in order to calculate the temperature at sea-level or the climatological mean annual temperature (MAT_clim). The experiment excluding the isostasy feedback has a MAT_clim about 0.5˚C lower than the standard experiment before the onset to full glaciation occurs, because of differences in the surface albedo (Figure 9). After the transition to the continental scale ice sheet, this difference becomes negligible because the area of the continental scale ice sheet is bounded by the size of the Antarctic continent and is nearly the same in both simulations. The initial temperature difference between 1150 and 1000 ppmv is due to the larger ice sheet area in the experiment that excludes the isostasy feedback. The larger the ice sheet area, the more incoming solar radiation will be reflected and the lower the surface temperature. The difference in the elevation corrected MAT_clim threshold to full glaciation is ~2˚C.

https://doi.org/10.5194/egusphere-2023-399
Preprint. Discussion started: 17 March 2023

4 Threshold dependency on orbital forcing

Ice sheet hysteresis occurs when a threshold in the forcing is crossed that leads to a positive feedback loop. On palaeoclimatic timescales on the order of 100 kyr and longer, this threshold is determined by changes in the carbon cycle (or changes in the atmospheric CO_2 concentration) and variations in the orbital parameters. First, the influence of the eccentricity is evaluated because the eccentricity modulates the magnitude of the precession and hence determines the magnitude of a threshold (Section 4.1).Then, simulations are run to a steady-state for a constant forcing for different orbital parameter combinations (Section 4.2).

4.1 Influence of the eccentricity

There exists a CO_2 threshold to continental scale glaciation for a certain bedrock topography. However, in a narrow range of CO_2 concentrations, the glaciation threshold is paced by the orbital parameters. Fig. 10 shows the eccentricity thresholds to continental-scale glaciation for a constant CO_2 forcing between 810 ppmv and 890 ppmv and the eccentricity thresholds for complete deglaciation for a CO_2 forcing between 980 and 1060 ppmv. The time axis indicates the duration since the start of the simulations and shows the change in sensitivity of the ice sheet to the forcing due to changing initial conditions (i.e. the ice sheet size has changed after a few precessional cycles). For atmospheric CO_2 values below 810 ppmv, the ice sheet always grows to a continental scale when the eccentricity declines below 0.04. For CO_2 values exceeding 890 ppmv, the ice sheet cannot grow to a continental scale, not even during a prolonged insolation minimum. In this narrow range of CO_2 concentrations, the eccentricity has a large influence on the ice sheet initiation and stability. Starting from a bare bedrock, the ice sheet stops growing and either declines or stays with constant volume whenever the eccentricity exceeds a value of 0.05 and then grows again when eccentricity declines. The ice sheet can initially grow and vary with the precession for up to four cycles before the onset to full glaciation sets in, depending on the value for the eccentricity and the CO_2 forcing.

The extreme eccentricity value of 0.063 that occurs after 2 Myr is not sufficient to melt the ice sheet once it has grown to a continental scale. This shows again the hysteresis effect of the Antarctic ice sheet: an eccentricity exceeding 0.03 is enough for preventing the ice sheet from growing to a continental scale at 890 ppmv, while an eccentricity of >0.06 is not sufficient to make the ice sheet melt entirely again. The extreme eccentricity of 0.063 influences the ice sheet volume for all simulations forced with a constant CO_2 concentration between 800 and 890 ppmv, but the peak insolation forced by the precessional cycle is too short-lived to melt the entire ice sheet. Such extreme values of the eccentricity exceeding 0.06 only occur when the 100 kyr cycle, the 405 kyr cycle and the 2.4 Ma cycle reach a maximum. The absolute maximum in the eccentricity of 0.064 at 32.2 Ma and a minimum in the 2.4 Ma cycle around 33.4 Ma are captured in this interval, important for determining the respective thresholds to ice sheet decline and ice sheet growth.

https://doi.org/10.5194/egusphere-2023-399
Preprint. Discussion started: 17 March 2023

It is remarkable that it is not only the magnitude of the eccentricity that determines the timing of ice sheet growth, but also the initial size of the ice sheet that is determined by the ice sheet history. Even though the CO_2 forcing is constant, the ice sheet grows to a fully glaciated state consecutively for a CO_2 forcing of 850 ppmv, 860 ppmv, 870 ppmv, 880 ppmv and 890 ppmv. The higher the CO_2 concentration, the more the ice sheet needs to grow before the threshold to full glaciation is reached.

Starting from a fully glaciated continent, the CO_2 threshold to complete deglaciation has a range between 980 and 1060 ppmv (Figure 10). An eccentricity of >0.05 initiates ice sheet melt in a CO_2 concentration range between 1020 and 1060 ppmv. Either a higher value for the eccentricity or a longer duration since the start of the experiments is needed to melt the Antarctic ice sheet for lower CO_2 values. The experiment duration has an influence on the initial size of the ice sheet. For instance, the eccentricity maximum of 0.051 at the start of the experiment was not high enough to melt the Antarctic ice sheet at a CO_2 forcing of 1050 ppmv. However, the ice sheet declines during the next eccentricity maximum exceeding 0.038 for a CO_2 forcing of 1050 ppmv, while it can regrow for a CO_2 forcing of 1040 ppmv. This indicates that the CO_2 and orbital parameter thresholds exhibit state-dependency; the thresholds to glaciation or deglaciation differ depending on the initial size of the ice sheet. The extreme eccentricity of 0.063 also induces the deglaciation at CO_2 concentrations between 980 ppmv and 1010 ppmv.

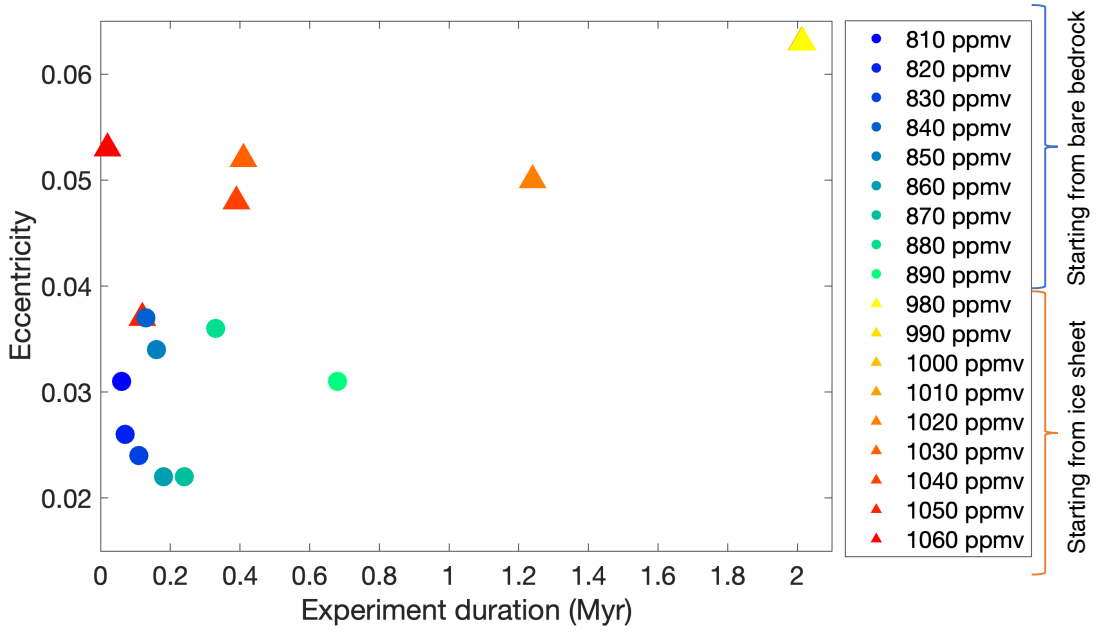

Figure 10: Eccentricity thresholds for ice sheet initiation starting from a bare bedrock (blue to green dots) and eccentricity thresholds for ice sheet decline (red to yellow triangles) for a range of different CO_2 values. The time on the x-axis indicates the duration before the continental-scale ice sheet growth or the ice sheet decline initiates. The experiment duration has an influence on the initial size of the ice sheet before another threshold is reached. The thresholds are determined using the Wilson maximum bedrock topography.

https://doi.org/10.5194/egusphere-2023-399
Preprint. Discussion started: 17 March 2023

4.2 Constant forcing runs for different orbital parameter combinations

So far, the hysteresis effect is investigated with a time-dependent forcing. To further separate the effects of the orbital parameters and the CO_2 thresholds on glaciation and deglaciation, a number of simulations are run to a steady-state for a constant forcing. Three different summer insolation (mean for DJF at 65˚S) values are selected to perform the steady-state runs: a relative low summer insolation of 427 Wm^{-2} (further referred to as a 'cold' orbital configuration), a relative high summer insolation of 467 Wm^{-2} (further referred to as a 'warm' orbital configuration) and an insolation value in between these two extremes of 440 Wm^{-2} (Figure 11). These insolation values can be achieved for different orbital parameter combinations, but correspond here to the values given in Table 3. The cold orbital configuration is chosen as the maximum insolation in an interval of ~40 kyr. This is about the time needed to grow a continental-scale ice sheet. The summer insolation is much lower during shorter intervals of several millennia, but these intervals are too short to significantly increase the size of the Antarctic ice sheet and to induce a continental scale glaciation. Fig. 11 also indicates that a warm orbital configuration in Antarctica can either be caused by a high obliquity or a high eccentricity in combination with the Earth in perihelion. The highest peak in the summer insolation at 31.18 Ma occurs when both eccentricity and obliquity are high. The selected cold orbital configuration occurs at a time that the eccentricity reaches a minimum.

Table 3: Austral summer insolation values, eccentricity and obliquity for the different selected orbital configurations.

Orbital configuration	Insolation (DJF-65˚S)	Eccentricity	Obliquity
'cold'	427 Wm^2	0.017	22.5˚
'intermediate'	440 Wm^2	0.022	23.2˚
'warm'	467 Wm^2	0.049	23.3˚

https://doi.org/10.5194/egusphere-2023-399
Preprint. Discussion started: 17 March 2023

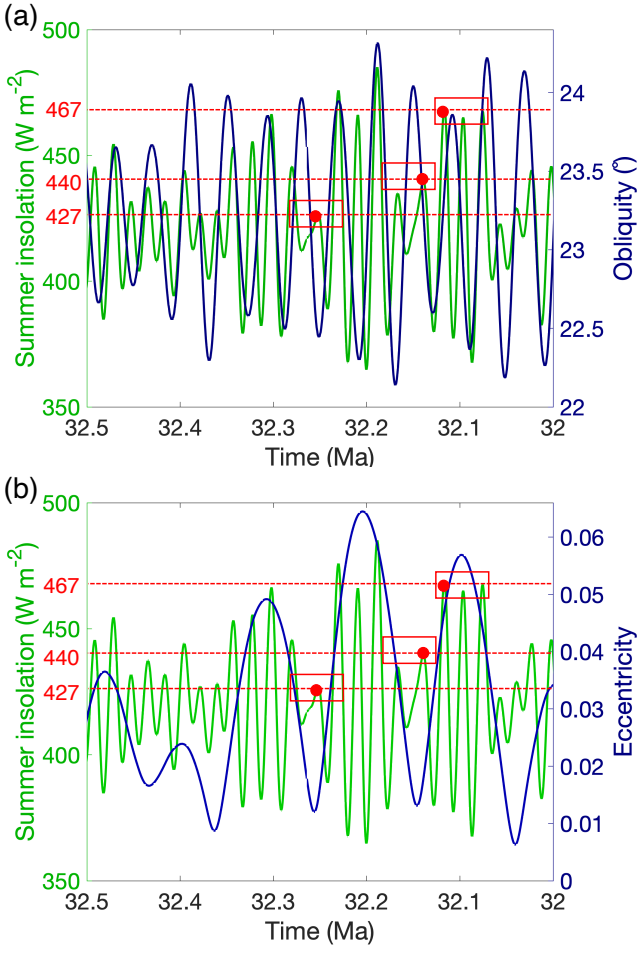

Figure 11: Summer insolation variations at 65°S with respect to the (a) obliquity and (b) eccentricity. Three different summer insolation values are indicated by the red dots that indicate the maximum insolation during a 40 kyr interval. These three different insolation values are representative for a relative cold orbital configuration (427 Wm^{-2}), an intermediate orbital configuration (440 Wm^{-2}) and a warm orbital configuration (467 Wm^{-2}).

Starting from a bare bedrock, the Antarctic ice sheet can grow to a continental scale for our cold orbital configuration for a CO_2 forcing up to 850 ppmv (Figure 12a). For an intermediate orbital configuration, the ice sheet can grow to a continental scale up to a CO_2 forcing of 700 ppmv and for a warm orbit, the ice sheet is never able to grow beyond a critical threshold to induce continental scale ice sheet growth. Starting from a fully glaciated continent, the Antarctic ice sheet declines for a CO_2 forcing of 1000 ppmv and higher (Figure 12b). The ice sheet never completely deglaciates during a cold orbit or an intermediate orbit in the range of considered CO_2 concentrations.

https://doi.org/10.5194/egusphere-2023-399
Preprint. Discussion started: 17 March 2023

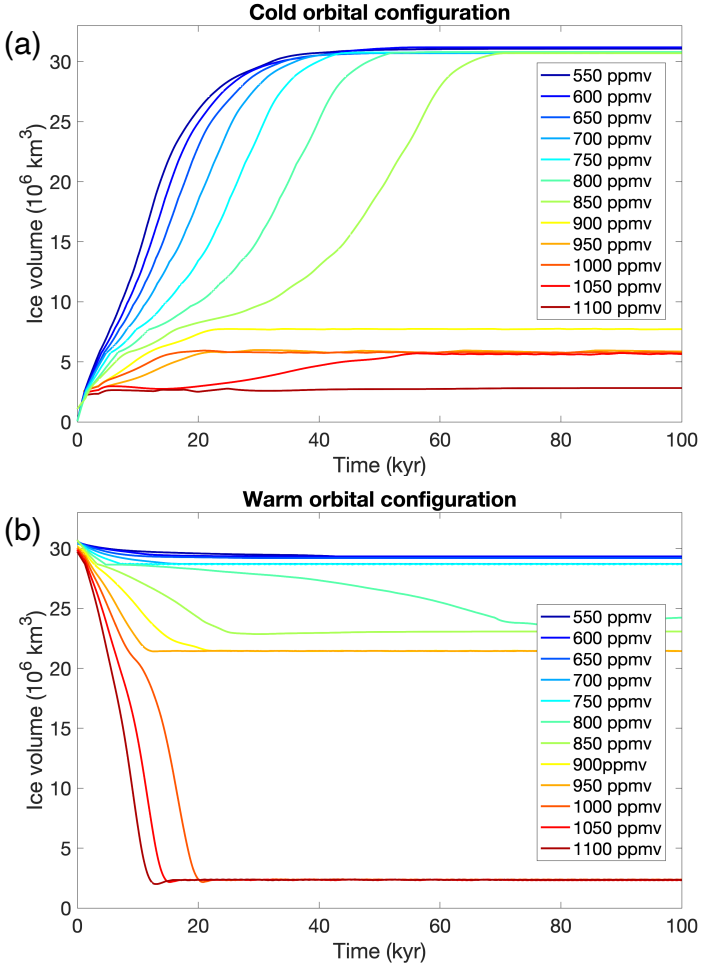

370 **Figure 12: Ice sheet evolution until steady-state for different constant forcing scenarios. (a) A cold orbital configuration (summer insolation at 65°S of 427 Wm^{-2}) and different CO_2 concentrations at interval of 50 ppmv starting from a bare bedrock. (b) A warm orbital configuration (summer insolation at 65°S of 467 Wm^{-2}) and different CO_2 concentrations at an interval of 50 ppmv starting from a fully glaciated continent.**

375 The timescales of growing and melting a continental ice sheet reveal an asymmetry. It takes about 30-70 kyr to build-up a continental scale Antarctic ice sheet, while melting the ice sheet takes about 10-20 kyr. The ice sheet grows much faster to a continental scale for a CO_2 forcing of 550 ppmv than for a CO_2 forcing of 850 ppmv, because the initial area of positive mass balance is much larger (Figure 13). A CO_2 concentration of 850 ppmv is close to the glaciation threshold and ice sheet-climate feedbacks are necessary to make the ice sheet grow. Initially, the ice sheet grows fast up to 18 kyr when the ice sheet volume
380 change stagnates and increases again after 30 kyr when the ice sheet covers about one third of the Antarctic continent and the ice-albedo and height-mass balance feedback reinforce the ice sheet growth. The highest mass balance rates occur along the

https://doi.org/10.5194/egusphere-2023-399
Preprint. Discussion started: 17 March 2023

ice sheet margin and range between 2-4 m yr^{-1} accumulation. During the early stage of ice sheet build-up, the accumulation in the Gamburtsev Mountains goes up to 0.5 m yr^{-1}, while it is around 2 m yr^{-1} in Dronning Maud Land. As the ice sheet grows, the accumulation lowers in central Antarctica, somewhat similar to today due to the development of a high-pressure area.

385

The "coldest" orbital configuration, thus corresponding to the lowest austral summer insolation occurs when the obliquity is low, the eccentricity is high, and the Earth is in aphelion. The time-dependent results clearly suggest that the eccentricity must largely determine the ice sheet growth because the time scale to initiate continental-scale glaciation is longer than the period of the precession or obliquity for the higher CO_2 concentrations. The CO_2 threshold to induce a glaciation in a transient setting
390 is therefore lower for high values of the eccentricity. Fig. 14a shows the maximum ice sheet volume for simulations starting from a bare bedrock for a constant CO_2 concentration and a constant eccentricity (while precession and obliquity are varying). Fig. 14b shows the maximum ice sheet volume for simulations starting from a bare bedrock for a constant CO_2 concentration and a constant obliquity (while precession and eccentricity vary). Figs. 14c and 14d show the minimum ice sheet volume for similar runs, but starting from a continental scale ice sheet.

395

The higher the eccentricity, the lower is the CO_2 concentration to induce the deglaciation (Figure 14c). On the other hand, for a given CO_2 forcing below the glaciation threshold, the ice sheet can grow more for a higher eccentricity (Figure 14a). The higher eccentricity modulates the precession and for a high eccentricity the summer insolation minimum is lower when the Earth is in aphelion. As noticed earlier, the duration of such a very low insolation minimum is not long enough to make the
400 ice sheet grow on the entire Antarctic continent and therefore, at high values for the eccentricity the CO_2 concentration needs to drop more to initiate ice sheet growth. Fig. 14 also shows hysteresis behaviour, where the existence of a large ice sheet for a given forcing is dependent on the initial presence or absence of an ice sheet.

https://doi.org/10.5194/egusphere-2023-399
Preprint. Discussion started: 17 March 2023

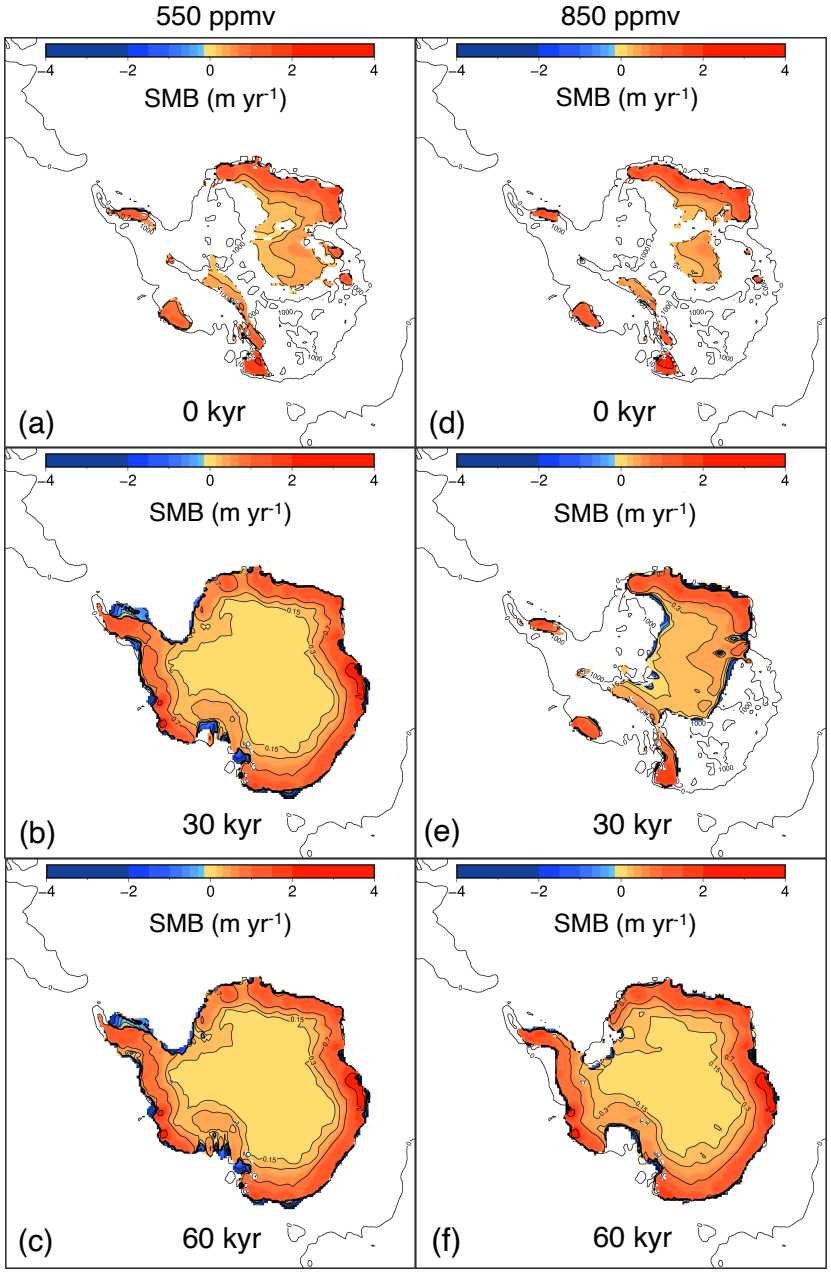

405

Figure 13: Antarctic ice sheet surface mass balance (SMB) for the simulation starting from a bare bedrock forced by a cold orbital configuration and a CO_2 concentration of 550 ppmv after (a) 0 kyr, (b) 30 kyr, (c) 60 kyr and a CO_2 concentration of 850 ppmv after (d) 0 kyr, (e) 30 kyr, (f) 60 kyr.

410

https://doi.org/10.5194/egusphere-2023-399
Preprint. Discussion started: 17 March 2023

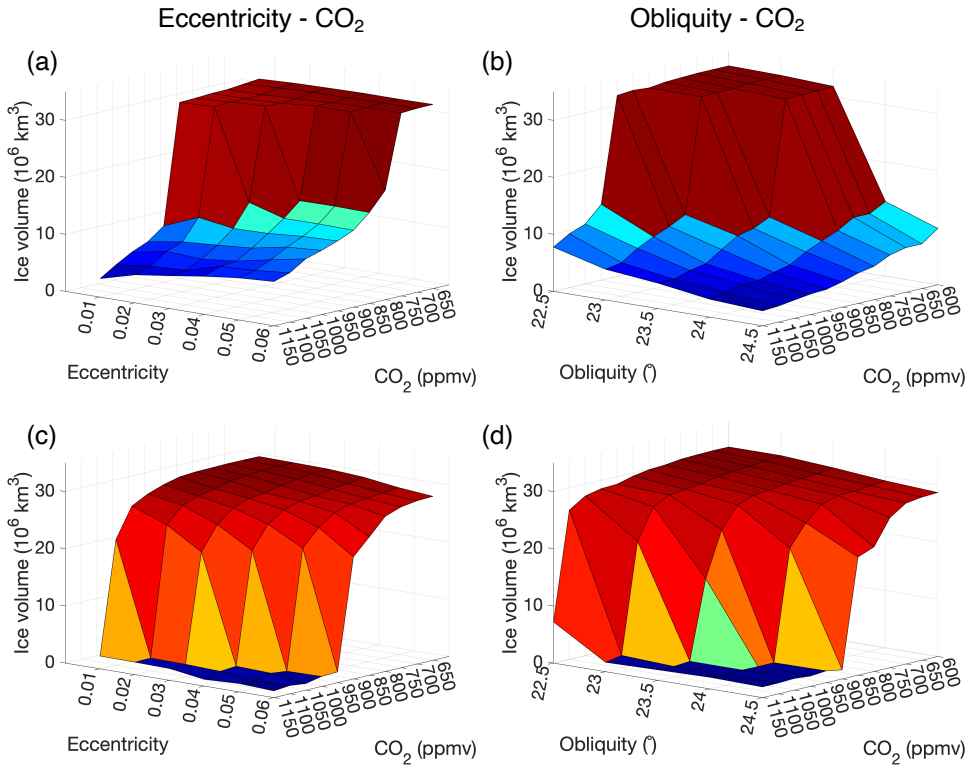

Figure 14: Simulations starting from a bare bedrock showing the maximum ice sheet volume for a range in CO_2 concentrations between 600 ppmv and 1150 ppmv for (a) a constant eccentricity between 0.01 and 0.06, while precession and obliquity are variable and (b) a constant obliquity between 22.5˚ and 24.5˚, while precession and eccentricity are variable. (c) and (d) are the same as (a) and (b), but the simulations start from a continental scale ice sheet and the minimum ice sheet volume achieved during the run is shown.

Fig. 14b shows the maximum ice sheet volume for simulations starting from a bare bedrock for a constant obliquity and a constant CO_2 concentration, while Fig. 14d shows the minimum ice sheet volume for similar runs starting from a continental scale ice sheet. The lower values for the obliquity clearly favour glaciation. For a constant obliquity of 22.5˚, the ice sheet grows to a continental scale at 1000 ppmv, while for an obliquity of 24.5˚, the ice sheet never reaches the continental scale. For the simulations starting from a continental scale ice sheet, the ice sheet never completely melts for a low obliquity of 22.5˚, not even for a high CO_2 forcing of 1150 ppmv. This indicates that the role of the eccentricity for melting a large-scale ice sheet is only important during times that the obliquity is high. Looking at the transition between a glaciated and a deglaciated continent for a constant forcing, it is apparent that the ice sheet volume first gradually changes before a strong nonlinear feedback initiates. This effect is further investigated simulating steady state ice sheet geometries for a range in temperature anomalies starting again from either and ice-free continent or bare bedrock and starting from an ice sheet (Figure 15). Starting

https://doi.org/10.5194/egusphere-2023-399
Preprint. Discussion started: 17 March 2023

from the glaciated continent, first the ice sheet retreats with ~40% of the continental-scale ice sheet area before the non-linear feedbacks are initiated. On the other hand, when starting from a bare bedrock, the steady-state ice sheet area first gradually increasing when lowering the surface temperature until the ice continent is covered with approximately 40% ice before a sharp transition occurs towards a fully glaciated continent.

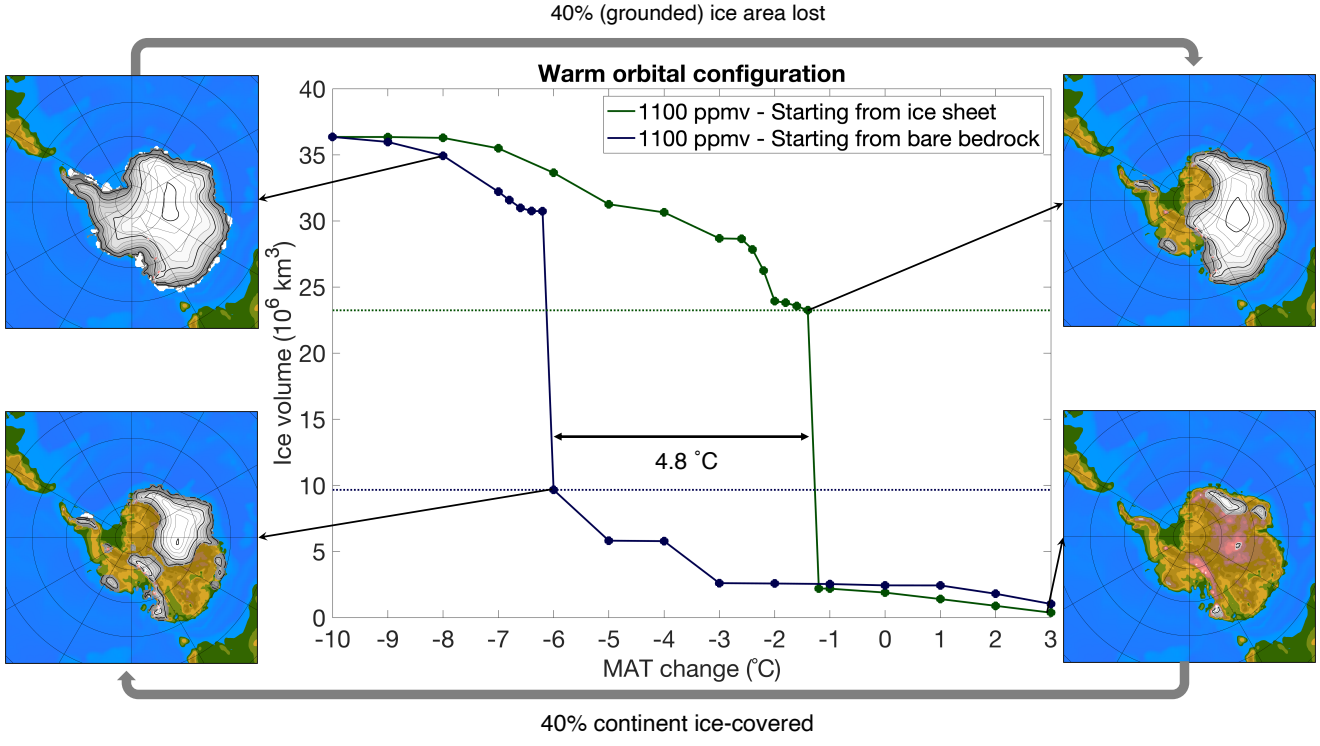

Figure 15: Steady-state ice sheet volume for a range in mean annual temperature perturbation thresholds for ice sheet growth and decline for a warm orbital configuration of 467 Wm^{-2} at 65˚S and a constant CO_2 concentrations of 1100 ppmv. The green horizontal dotted line indicates the ice sheet volume at which the strong nonlinear ice sheet decline initiates. The ice sheet volume at which a strong nonlinear increase ice sheet growth initiates is indicated by the blue horizontal dotted line. Snapshot of the ice sheet geometry are given at the tipping points.

5 Discussion

Hysteresis behaviour related to the build-up and decline of ice sheets has a geometric cause (Oerlemans, 2002). The snowline must lower to allow for a snow cover to develop over most of the topography to initiate ice build-up. Obviously, the transition would be sharpest when the topography is flat and the snowline would intersect the entire topography at once. The lowering of the ice sheet surface during decay causes the atmospheric temperatures to rise even more because of the lapse rate and

https://doi.org/10.5194/egusphere-2023-399
Preprint. Discussion started: 17 March 2023

accelerates the melting process, a process named the height-mass balance feedback. Because hysteresis has very much a geometrical origin, the initial height of the bedrock topography and the height of the continental-scale ice sheet are of crucial importance to determine the thresholds for glaciation and deglaciation. We have confirmed that the CO_2 thresholds and especially temperature thresholds to initiate and terminate glaciations differ depending on the height of the bedrock.

The hysteresis effect in our simulations has a magnitude of about 170-180 ppmv, slightly depending on the bedrock topography. The transition occurs as a sudden, nonlinear response when the ice-albedo feedback and height-mass balance feedback reinforce the ice sheet growth at the threshold value. An additional positive feedback arises from the increased ice flow for warmer ice. It is suggested that albedo feedbacks between the ice sheet and the climate increase the strength of the hysteresis. Pollard and DeConto (2005) found a hysteresis effect of about 100 ppmv at the EOT, using a matrix look-up table with few initial ice sheet geometries that only roughly captured the ice-albedo feedback. Their hysteresis curves also showed a more stepwise change towards full glaciation and deglaciation. This is because mainly the height-mass balance feedback strengthens the ice sheet growth each time the topography is above the snowline, and the continent partly glaciates.

Our simulations indicate that the ice sheet-climate feedbacks cause rapid ice sheet expansion when the ice sheet covers about 40% of the continent (Figure 15). Oppositely, the Antarctic ice sheet area needs to decrease by about 40% (corresponding to an ice volume loss of 30% of the grounded ice volume) to initiate rapid ice sheet decay. A similar geometrical threshold is also found for melting of the present-day Greenland ice sheet. In their study, Ridley et al. (2010) state that the ice-albedo feedback becomes very effective when the ice sheet volume loss is about 30%. Mikolajewicz et al. (2007) found that a changing surface albedo due to ice melting increased the local temperatures by up to 10˚C in summer time. The sharp glacial-deglacial transitions are caused by both the ice-albedo feedback and the height-mass balance feedback and it is thought that their impact on the surface temperatures are of equal magnitude (Ridley et al., 2005). Opposite to the sharp transition between glacial and deglacial states from our study, studies that neglect the ice-albedo feedback such as Huybrechts (1994b) and Garbe et al. (2020) show a more gradual transition towards a deglaciated continent. Therefore, these studies might also overestimate the temperature forcing needed to melt the present-day Antarctic ice sheet.

The solid Earth rebound acts as a negative feedback during the glaciation of the Antarctic continent. Our simulations show that the strength of this feedback is quite large and lowers the CO_2 threshold to continental scale glaciations by about 130 ppmv. Oerlemans (2002) initially stated that the influence of isostatic movements should be small because the glaciation threshold occurs when the ice sheet is still small. However, our simulations indicate that the combined effect of a higher surface elevation and more extensive albedo changes due to a larger area make a substantial difference in the glaciation threshold. For the present-day Antarctic ice sheet, the solid Earth uplift feedback has a stabilizing effect on the Antarctic ice sheet evolution since at least the last 10 kyr (Kingslake et al., 2018). Also for future projections of the Antarctic ice sheet on multi-centennial

https://doi.org/10.5194/egusphere-2023-399
Preprint. Discussion started: 17 March 2023

timescales, the uplift provides a negative feedback to future West Antarctic ice sheet loss by grounding line stabilization (Larour et al., 2019).

Non-linear ice sheet dynamics are also triggered by the orbital parameters. The eccentricity has a main influence on the initiation and termination of glaciations on the Antarctic continent with initiation during eccentricity minima and terminations during eccentricity maxima. This is somewhat surprisingly because the eccentricity only influences the forcing by modulating the precession. However, because the ice sheet decline depends on crossing a threshold value, the amplitude of the precession cycle is important which is governed by the eccentricity. Large values for the eccentricity result in a very low summer insolation during austral summer when the Earth is in aphelion and a very high summer insolation during austral summer when the Earth is in perihelion. To build up a continental scale Antarctic ice sheet, the role of the eccentricity is important to keep the amplitude of the precession low. Abe-Ouchi and Blatter (1993) indicated already that the periods of precession (~20 kyr) and obliquity (~40 kyr) are too short to build-up large ice sheets when the accumulation rate is low and therefore, eccentricity has to be low to prevent the summer insolation to peak when the Earth is in perihelion.

6 Conclusions

The early Cenozoic Antarctic ice sheet grew non-linearly during the late Eocene to Oligocene, when thresholds in the climate system were crossed. These thresholds at which glaciation occurs depends on the boundary conditions such as the bedrock elevation. The CO_2 threshold to glaciation is ~650 ppmv for the minimum bedrock elevation and ~870 ppmv for the maximum bedrock elevation datasets used in this study. The hysteresis behaviour of ice sheets arises because of the positive feedbacks associated with ice sheet growth and decline such as the elevation-surface mass balance feedback and the ice-albedo feedback. The Antarctic ice sheet hysteresis effect is independent of the specific bedrock elevation dataset and is ~180 ppmv or equivalent to a 4˚C to 5˚C regional mean annual temperature change. Our simulations indicate the need to include ice-albedo feedbacks when the ice sheet is replaced by tundra during ice sheet melting and oppositely during ice sheet growth. The rapid transition between glacial and deglacial states as found in our simulations is attributed to this ice-albedo feedback and sets in when the Antarctic continent covers about 40% of the area (threshold to glaciation) or when the ice area decreases with 40% of the total ice area (threshold to deglaciation).

An important stabilising feedback is the isostatic depression of the bedrock when the ice sheet is building up. When the ice sheet is growing, the bedrock is depressed because of the weight of the overlying ice and the surface elevation is lowered. When this feedback is neglected, the ice sheet grows much faster to a continental scale and the hysteresis effect is significantly weaker. We found that this feedback is significant because of both an increased surface elevation and a larger ice sheet accumulation area that lowers the surface albedo.

https://doi.org/10.5194/egusphere-2023-399
Preprint. Discussion started: 17 March 2023

The orbital parameters might regulate ice sheet growth and decline close to the CO_2 threshold of continental scale (de)glaciation. Especially the role of the eccentricity is large because ice sheet growth operates on a timescale of 30-70 kyr (longer than the precession and obliquity cycles) and ice sheet decline is initiated by crossing a threshold where the eccentricity determines the magnitude of this threshold value. The orbital parameters trigger both glaciations and deglaciations in a CO_2 range of ~80 ppmv.

Code and data availability

The code for the coupler CLISEMv1.0 used for the ice sheet-climate model simulations is available on Zenodo: https://doi.org/10.5281/zenodo.5245156 (Van Breedam et al.,2021b). All data used in this paper are available upon request.

Author contributions

JVB designed the coupling method between the emulator and the ice sheet model and developed the methodology and ran the simulations . MC developed the Gaussian process emulator and advised with the implementation of the ice sheet model component. PH developed the ice sheet model code and assisted to interpret the results throughout the entire process. JVB wrote the manuscript with contributions from all co-authors.

Competing interests

The authors declare that they have no conflict of interest.

Acknowledgement

Jonas Van Breedam acknowledges support from project G091820N, funded by the Research Foundation Flanders (FWO Vlaanderen). Michel Crucifix is funded as Research Director with the Belgian National Fund of Scientific Research FNRS.

References

Abe-Ouchi, A. and Blatter, H.: On the initiation of ice sheets, Annals of Glaciology, 18, 203-207, https://doi.org/10.3189/S0260305500011514, 1993.

Abe-Ouchi, A., Saito, F., Kawamura, K., Raymo, M. E., Okuno, J., Takahashi, K. and Blatter, H.: Insolation-driven 100,000 year glacial cycles and hysteresis of ice-sheet volume, Nature, 500, 190-193, https://doi.org/10.1038/nature12374, 2013.

Armstrong McKay, D. I., Staal, A., Abrams, J. F., Winkelmann, R., Sakschewski, B., Loriani, S., Fetzer, I., Cornell, S. E.,

https://doi.org/10.5194/egusphere-2023-399
Preprint. Discussion started: 17 March 2023

Rockström, J. and Lenton, T. M.: Exceeding 1.5˚C global warming could trigger multiple climate tipping points, Science, 377, https://doi.org/10.1126/science.abn7950, 2022.

Baatsen, M., van Hinsbergen, D. J. J., von der Heydt, A. S., Dijkstra, H. A., Sluijs, A., Abels, H. A., and Bijl, P. K.: Reconstructing geographical boundary conditions for palaeoclimate modelling during the Cenozoic, Clim. Past, 12, 1635–1644, https://doi.org/10.5194/cp-12-1635-2016, 2016.

Boers, N. and Rypdal, M.: Critical slowing down suggests that the western Greenland Ice Sheet is close to a tipping point, PNAS, 118, e2024192118, https://doi.org/10.1073/pnas.2024192118, 2021.

Calov, R. and Ganopolski, A.: Multistability and hysteresis in the climate-cryosphere system under orbital forcing, Geophysical Research Letters, 32, L21717, https://doi.org/10.1029/2005GL024518, 2005.

Cox, P.M., Betts, R.A., Bunton, C.B., Essery, R.L.H., Rowntree, P.R. and Smith. J.: The impact of new land surface physics on the GCM simulation of climate and climate sensitivity, Climate Dynamics, 15, 183-203, https://doi.org/10.1007/s003820050276, 1999.

Crucifix, M., Loutre, M. F., Lambeck, K. and Berger A.: Effect of isostatic rebound on modelled ice volume variations during the last 200 kyr, Earth and Planetary Science Letters, 184, 623-633, https://doi.org/10.1016/S0012-821X(00)00361-7, 2001.

De Vleeschouwer, D., Da Silva, A. C., Sinnesael, M., Chen, D., Day, J. E., Whalen, M. T., Guo, Z. and Claeys, p.: Timing and pacing of the Late Devonian mass extinction event regulated by eccentricity and obliquity, Nat Commun, 8, 2268, https://doi.org/10.1038/s41467-017-02407-1, 2017.

Garbe, J., Albrecht, T., Levermann, A., Donges, J. F. and Winkelmann, R.: The hysteresis of the Antarctic Ice Sheet, Nature, 585, 538-544, https://doi.org/10.1038/s41586-020-2727-5, 2020.

Horton, D. E., Poulsen, C. J., Montañez, I. P. and DiMichele, W. A.: Eccentricity-paced late Paleozoic climate change, Palaeogeography, Palaeoclimatology, Palaeoecology, 331-332, 150-161, https://doi.org/10.1016/j.palaeo.2012.03.014, 2012.

Houben, A. J. P., Bijl, P. K., Sluijs, A., Schouten, S. and Brinkhuis, H.: Late Eocene Southern Ocean cooling and invigoration of circulation preconditioned Antarctica for full-scale glaciation. Geochemistry, Geophysics, Geosystems, 20, 2214–2234, https://doi.org/10.1029/2019GC008182, 2019.

Huybrechts, P.: Formation and disintegration of the Antarctic ice sheet, Annals of glaciology, 20, 336-340, https://doi.org/10.3189/1994AoG20-1-336-340, 1994.

Huybrechts, P. and De Wolde, J.: The Dynamic Response of the Greenland and Antarctic Ice Sheets to Multiple-Century Climatic Warming, J. Clim., 12, 2169–2188, https://doi.org/10.1175/1520-0442(1999)012<2169:tdrotg>2.0.co;2, 1999.

Huybrechts, P.: Sea-level changes at the LGM from ice-dynamic reconstructions of the Greenland and Antarctic ice sheets during the glacial cycles. Quaternary Science Reviews, 21, 1-3, 203-231, https://doi.org/10.1016/S0277-3791(01)00082-8, 2002.

Janssens, I. and Huybrechts, P.: The treatment of meltwater retention in mass-balance parameterizations of the Greenland ice sheet, Ann. Glaciol, 31, 133-140, https://doi.org/10.3189/172756400781819941, 2000.

Kennett, J. P.: Cenozoic evolution of Antarctic glaciation, the circum-Antarctic Ocean, and their impact on global

paleoceanography, J. Geophys. Res., 82, 3843-3860, https://doi.org/10.1029/JC082i027p03843, 1977.

Kingslake, J., Scherer, R. P., Albrecht, T., Coenen, J., Powell, R. D., Reese, R., Stansell, N. D., Tulaczyk, S., Wearing, M. G. and Whitehouse, P. L.: Extensive retreat and re-advance of the West Antarctic Ice Sheet during the Holocene, Nature, 558, 430-434, https://doi.org/10.1038/s41586-018-0208-x, 2018.

Klose, A. K., Karle, V., Winkelmann, R. and Donges, J. F.: Emergence of cascading dynamics in interacting tipping elements of ecology and climate, R. Soc. Open Sci., 7, 200599, http://dx.doi.org/10.1098/rsos.200599, 2020.

Larour, E., Seroussi, H., Adhikari, S., Ivins, E., Caron, L., Morlighem, M. and Schlegel, N.: Slowdown in Antarctic mass loss from Solid Earth and sea-level feedbacks, Science, 364, eaav7908, https://doi.org/10.1126/science.aav7908, 2019.

Laskar, J., Robutel, P., Joutel, F., Gastineau, M., Correia, A.C.M. and Levrard, B.: A long-term numerical solution for the insolation quantities of the Earth, Astron. Astrophys., 428, 261-285, https://doi.org/10.1051/0004-6361:20041335, 2004.

Laskar, J., Fienga, A., Gastineau, M. And Manche, H.: La2010: a new orbital solution for the long-term motion of the Earth, Astronomy & Astrophysics, 532, A89, https://doi.org/10.1051/0004-6361/201116836, 2011.

Lenton, T., Rockström, J., Gaffney, O., Rahmstorf, S., Richardson, K., Steffen, W. and Schellnhuber, H. J.: Climate tipping points – too risky to bet against, Nature, 575, 592-595, https://doi.org/10.1038/d41586-019-03595-0, 2019.

Letréguilly, A., Huybrechts, P. and Reeh, N.: Steady-state characteristics of the Greenland ice sheet under different climates, Journal of glaciology, 37, 149-157, https://doi.org/10.3189/S0022143000042908, 1991.

Levermann, A. and Winkelmann, R.: A simple equation for the melt elevation feedback of ice sheets, The Cryosphere, 10, 1799–1807, https://doi.org/10.5194/tc-10-1799-2016, 2016.

Mikolajewicz, U., Vizcaíno, M., Jungclaus, J. and Schurgers, G.: Effect of ice sheet interactions in anthropogenic climate change simulations, Geophys. Res. Lett., 34, L18706, https://doi.org/10.1029/2007GL031173, 2007.

Mitchell, R. N., Gernon, T. M., Cox, G. M., Nordsvan, A. R., Kirscher, U., Xuan, C., Liu, Y. and He, X.: Orbital forcing of ice sheets during snowball Earth, Nat. Commun., 12, 4187, https://doi.org/10.1038/s41467-021-24439-4, 2021.

Oerlemans, J.: On glacial inception and orography, Quaternary International, 95-96, 5-10, https://doi.org/10.1016/S10406182(02)00022-8, 2002.

Pagani, M., Huber, M., Zhonghui, L., Bohaty, S. M., Henderiks, J., Sijp, W., Krishnan, S. and DeConto, R.M.: The Role of Carbon Dioxide During the Onset of Antarctic Glaciation, Science, 334, 1261-1264, https://doi.org/10.1126/science.1203909, 2011.

Payne, A. J., Nowicki S., Abe-Ouchi, A., Agosta, C., Alexander, P., Albrecht, T., Asay-Davis, X., Aschwanden, A., Barthel, A., Bracegirdle, T. J., Calov, R., Chambers, C., Choi, Y., Cullather, R., Cuzzone, J., Dumas, C., Edwards, T., Felikson, D., Fettweis, X., Galton-Fenzi, B. K., Goelzer, H., Gladstone, R., Golledge, N. R., Gregory, J. M., Greve, R., Hatterman, T., Hoffman, M. J., Humbert, A., Huybrechts, P., Jourdain, N. C., Kleiner, T., Larour, E., Le clec'h, S., Lee, V., Leguy, G., Lipscomb, W. H., Little, C. M., Lowry, D., Morlighem, M., I. Nias, Pattyn, F., Pelle, T., Price, S. F., Quiquet, A., Reese, R., Rückamp, M., Schlegel, N-J., Seroussi, H., Shepherd, A., Simon, E., Slater, D., Smith, R., Straneo, F., Sun, S., Tarasov, L., Trusel, L.D., Van Breedam, J., van de Wal, R., van den Broeke, M., Winkelmann, R., Zhao, C., Zhang, T. and Zwinger, T.:

Future Sea Level Change Under Coupled Model Intercomparison Project Phase 5 and Phase 6 Scenarios From the Greenland and Antarctic Ice Sheets, Geophysical Research Letters, 48, e2020GL091741, https://doi.org/10.1029/2020GL091741, 2021.

Pollard, D. and DeConto, R. M.: Hysteresis in Cenozoic Antarctic ice-sheet variations, Global and Planetary Change, 45, 9 21, https://doi.org/10.1016/j.gloplacha.2004.09.011, 2005.

Pope, V. D., Gallani, M. L., Rowntree, P. R. and Stratton, R. A.: The impact of new physical parametrizations in the Hadley Centre climate model: HadAM3, Climate Dynamics, 16, 123-146, https://doi.org/10.1007/s003820050009, 2000.

Ridley, J. K., Huybrechts, P. and Gregory, J. M.: Elimination of the Greenland Ice Sheet in a High CO_2 Climate, Journal of Climate, 18, 3409-3427, https://doi.org/10.1175/JCLI3482.1, 2005.

Ridley, J., Gregory, J. M., Huybrechts, P. and Lowe, J.: Thresholds for irreversible decline of the Greenland ice sheet, Clim. Dyn., 35, 1065-1073, https://doi.org/10.1007/s00382-009-0646-0, 2010.

Robinson, A., Calov, R. and Ganopolski, A.: Multistability and critical thresholds of the Greenland ice sheet, Nature Clim. Change, 2, 429-432, https://doi.org/10.1038/nclimate1449, 2012.

Rosier, S. H. R., Reese, R., Donges, J. F., De Rydt, J., Gudmundsson, G. H., and Winkelmann, R.: The tipping points and early warning indicators for Pine Island Glacier, West Antarctica, The Cryosphere, 15, 1501–1516, https://doi.org/10.5194/tc-15-1501-2021, 2021.

Van Breedam, J., Goelzer, H., and Huybrechts, P.: Semi-equilibrated global sea-level change projections for the next 10 000 years, Earth Syst. Dynam., 11, 953–976, https://doi.org/10.5194/esd-11-953-2020, 2020.

Van Breedam, J., Huybrechts, P., and Crucifix, M.: A Gaussian process emulator for simulating ice sheet–climate interactions on a multi-million-year timescale: CLISEMv1.0, Geosci. Model Dev., 14, 6373–6401, https://doi.org/10.5194/gmd-14-6373-2021, 2021a.

Van Breedam, J., Huybrechts, P., and Crucifix, M.: CLimate Ice Sheet EMulator v1.0 (CLISEMv1.0), Zenodo [code], https://doi.org/10.5281/zenodo.5245156, 2021b.

Van Breedam, J., Huybrechts, P. and Crucifix, M.: Modelling evidence for late Eocene Antarctic glaciations, Earth and Planetary Science Letters, 586, 117532, https://doi.org/10.1016/j.epsl.2022.117532, 2022.

Van Hinsbergen, D. J. J., de Groot, L. V., van Schaik, S. J., Spakman, W., Bijl, P. K., Sluijs, A., Langereis, C. G. and Brinkhuis, H.: A Paleolatitude Calculator for Paleoclimate Studies, PLoS ONE, 10, e0126946, https://doi.org/10.1371/journal.pone.0126946, 2015.

Williams, K. D., Senior C. A., and Mitchell, J. F. B.: Transient Climate Change in the Hadley Centre Models: The Role of Physical Processes, Journal of Climate, 2659-2674, https://doi.org/10.1175/1520-0442(2001)014<2659:TCCITH>2.0.CO;2, 2001.

Wilson, D. S., Jamieson, S. R., Barrett, P. J., Leitchenkov, G., Gohl, K. and Larter, D.: Antarctic topography at the Eocene Oligocene boundary, Paleogeography, Paleoclimatology, Palaeoecology, 335-336, 24-34, https://doi.org/10.1016/j.palaeo.2011.05.028, 2012.

Zeitz, M., Reese, R., Beckmann, J., Krebs-Kanzow, U., and Winkelmann, R.: Impact of the melt–albedo feedback on the future

https://doi.org/10.5194/egusphere-2023-399
Preprint. Discussion started: 17 March 2023

evolution of the Greenland Ice Sheet with PISM-dEBM-simple, The Cryosphere, 15, 5739–5764, https://doi.org/10.5194/tc-15-5739-2021, 2021.